# Neutrophil extracellular traps persist at high levels in the lower respiratory tract of critically ill COVID-19 patients

Werner J.D. Ouwendijk[1]*, Matthijs P. Raadsen[1], Jeroen J.A. van Kampen[1], Robert M. Verdijk[2], Jan H. von der Thusen[2], Lihui Guo[3,4], Rogier A.S. Hoek[5], Johannes P.C. van den Akker[6], Henrik Endeman[6], Thomas Langerak[1], Richard Molenkamp[1], Diederik Gommers[6], Marion P.G. Koopmans[1], Eric C.M. van Gorp[1], Georges M.G.M. Verjans[1] and Bart L. Haagmans[1]

[1]Department of Viroscience, Erasmus MC, Rotterdam, The Netherlands

[2]Department of Pathology, Erasmus MC, Rotterdam, The Netherlands

[3]Department of Respiratory Medicine, Amsterdam UMC, University of Amsterdam, Amsterdam, The Netherlands

[4]Department of Experimental Immunology, Amsterdam Infection and Immune Institute, Amsterdam UMC, University of Amsterdam, Amsterdam, The Netherlands

[5]Department Pulmonary Medicine, Erasmus MC, Rotterdam, the Netherlands

[6]Department of Adult Intensive Care, Erasmus MC, Rotterdam, the Netherlands

**Summary:** Aberrant neutrophil extracellular trap (NET) formation is implicated in acute respiratory distress syndrome (ARDS) pathogenesis. We demonstrate that NETs are present in blood and persist at high levels in the lower respiratory tract of critically ill COVID-19 patients with ARDS.

.

© The Author(s) 2021. Published by Oxford University Press for the Infectious Diseases Society of America. All rights reserved. For permissions, e-mail: journals.permissions@oup.com.

Accepted Manuscript

## FOOTNOTE PAGE

- The authors have no conflicts of interest to declare.
- The department of Viroscience received support from the EU Horizon 2020 dedicated call for COVID-19 research, grant number 101003589 (RECOVER). The department of Pathology received support from ZonMw grant number 10430 01 201 0016. No financial support was received for this manuscript.
- This information has not been presented elsewhere.
- Correspondence and requests for reprints can be addressed to Werner J.D. Ouwendijk PhD, Department of Viroscience, Erasmus MC, PO Box 2040, 3000 CA, Rotterdam, The Netherlands. Email: w.ouwendijk@erasmusmc.nl

Accepted Manuscript

## ABSTRACT

SARS-CoV-2 induced lower respiratory tract (LRT) disease can deteriorate to acute respiratory distress syndrome (ARDS). Because the release of neutrophil extracellular traps (NETs) is implicated in ARDS pathogenesis, we investigated the presence of NETs and correlates of pathogenesis in blood and LRT samples of critically ill COVID-19 patients. Plasma NET levels peaked early after ICU admission and correlated with SARS-CoV-2 RNA load in sputum and levels of neutrophil-recruiting chemokines and inflammatory markers in plasma. Baseline plasma NET quantity correlated with disease severity, but was not associated with soluble markers of thrombosis nor with development of thrombosis. High NET levels were present in LRT samples and persisted during the course of COVID-19, consistent with the detection of NETs in bronchi and alveolar spaces in lung tissue from fatal COVID-19 patients. Thus, NETs are produced and retained in the LRT of critical COVID-19 patients and could contribute to SARS-CoV-2-induced ARDS pathology.

**Key words:** COVID-19, SARS-CoV-2, neutrophil extracellular traps, acute respiratory distress syndrome, neutrophils.

Accepted Manuscript

## BACKGROUND

Severe acute respiratory syndrome coronavirus 2 (SARS-CoV-2) has been identified as the causative agent of a global outbreak of respiratory tract disease (COVID-19) [1]. As of July 15th 2020, over 13.3 million COVID-19 cases and more than 578 thousand deaths were reported worldwide [2]. COVID-19 is characterized by range of symptoms including fever, cough, dyspnea and myalgia, but in some patients the infection results in viral pneumonia [3, 4]. About 18% of hospitalized patients develop acute respiratory distress syndrome (ARDS), requiring admission to the intensive care unit (ICU) and mechanical ventilation for a period of several weeks [3, 4].

Pulmonary (hyper)inflammatory responses and coagulopathy are major determinants of disease severity and death in COVID-19 patients [5, 6]. Neutrophils are key players in the pathogenesis of ARDS and have been found to extensively infiltrate lung tissue of COVID-19 patients as well [7, 8]. In addition to killing pathogens through oxidative burst and phagocytosis, neutrophils can produce neutrophil extracellular traps (NETs) – web-like structures of DNA, histones, antimicrobial proteins and oxidant enzymes [9]. Excessive NET formation is associated with ARDS triggered by a variety of viruses and bacteria [10-12], as well as hypercoagulability [13]. Recent studies demonstrated increased NET levels in plasma of hospitalized COVID-19 patients, as well as the presence of platelet-NET aggregates in plasma and affected lung tissue [14, 15]. Interestingly, plasma NET abundance appeared to correlate with disease severity in hospitalized COVID-19 patients [14, 15]. These results need to be confirmed in larger cohorts and compared to critically ill SARS-CoV-2 infected patients with ARDS. The aim of this prospective cohort study was to investigate the presence of NETs and correlates of pathogenesis

Accepted Manuscript

in blood and lower respiratory tract samples of critically ill COVID-19 patients with ARDS.

## METHODS

**Clinical samples and ethical statement.** Seventy-seven COVID-19 patients admitted to the ICU with ARDS at the Erasmus MC, Rotterdam, the Netherlands between 2 March and 20 April 2020 were included in a biobank study (CIUM) aimed at studying ARDS and sepsis in the ICU (Supplementary Table 1). CT pulmonary angiography was performed on all COVID-19 patients prior ICU admission based on a clinical scoring system (YEARS criteria). Upon ICU admission, all patients underwent CT pulmonary angiography, which was subsequently repeated at 7 days post admission, or if there was abrupt deterioration of the clinical condition of the patient. Plasma samples were obtained at time of admission at ICU until day 28 post-inclusion (days 1, 2, 7, 14, 21 and 28), for as long as the patient was in the ICU. Sputum, bronchiolar lavage (BL) and bronchoalveolar lavage (BAL) samples were obtained for diagnostic purposes and surplus material was used for this study. Patient care and research were conducted in compliance with Institutional guidelines and the Declaration of Helsinki. Due to the clinical state of most ARDS patients (*i.e.* intubated, comatose), deferred proxy consent was obtained instead of direct written informed consent from the patients. Retrospective written informed consent was obtained from patient after recovery. The study protocol was approved by the medical ethical committee of the Erasmus MC, Rotterdam, the Netherlands (MEC-2017-417 and MEC-2020-0222). Written informed consent for research use was obtained by the Sanquin Blood Bank (Rotterdam, the Netherlands) for plasma samples from anonymous healthy control subjects. The use of surplus BAL samples obtained from anonymized influenza pneumonia patients and lung transplant

Accepted Manuscript

patients (previously tested negative for NETs) was approved by the medical ethical committee of the Erasmus MC (MEC-2015-306). Informed consent was waived by the institutional privacy knowledge officer.

**SARS-CoV-2 RT-qPCR.** SARS-CoV-2 E gene copies per ml sample were determined by reverse-transcriptase linked quantitative PCR (RT-qPCR) as described [16].

**His-DNA and MPO-DNA ELISA.** Cell-free histone-DNA (his-DNA) complexes were analyzed using the Human Cell Death Detection ELISA$^{PLUS}$ (Sigma Aldrich), using 3,3',5,5'-Tetramethylbenzidine (TMB) as a substrate and measured at 450 nm, using 620 nm as reference. Myeloperoxidase (MPO)-DNA ELISA was performed as described [17]. In brief, wells were coated with mouse anti-MPO antibody (5 µg/ml; clone 4A4, Bio-Rad) overnight at 4˚C. Samples (40 µl) were mixed with incubation buffer and peroxidase-labelled anti-DNA antibody (80 µl/sample; both from the Human Cell Death Detection ELISA$^{PLUS}$ kit; Sigma Aldrich), incubated for 2 hours at room temperature and analyzed using TMB as a substrate. All samples presented in a single figure were measured on the same plate in the same assay.

**Immunohistochemistry.** Post-mortem lung tissues were obtained from 6 COVID-19 patients (Supplementary Table 1), fixed in formalin and embedded in paraffin. Tissue sections were analyzed by immunohistochemistry (IHC) using the following primary antibodies: mouse anti-SARS-CoV nucleoprotein (40143-MM05; Sino Biological), rabbit anti-MPO (A0398; Dako), mouse anti-CD61 (M0753; Dako), rabbit anti-citrullinated histone H3 (H3Cit; ab5103; Abcam) and rabbit anti-fibrinogen (F0111;

Accepted Manuscript

Dako). Tissue sections were deparaffinized, rehydrated, subjected to heat-induced antigen retrieval in Tris-EDTA buffer (pH = 9.0) or citrate buffer (pH=6.0), blocked and incubated with primary antibodies for 1 hour at room temperature or overnight at 4˚C. SARS-CoV nucleoprotein staining was performed by incubating sections with biotin-conjugated secondary goat anti-mouse or rabbit anti-goat IgG antibodies followed by horseradish peroxidase-conjugated streptavidin (Dako). Staining was visualized using 3-amino-9-ethylcarbazole (AEC), and sections were counterstained with hematoxylin (both: Sigma-Aldrich). Double chromogenic staining was performed using secondary polymer anti-rabbit or anti-mouse IgG AP and PermaRed and PermaBlue as substrates (Diagnostic Biosystem). Images of IHC staining were obtained by scanning the slides using the Nanozoomer 2.0 HT (Hamamatsu) or Olympus ColorView camera fitted onto an Olympus BX51 microscope using Olympus Cell A software.

**Detection of IL-6, IL-8 and CXCL10.** Quantification of interleukin-6 (IL-6), IL-8, and C-X-C motif chemokine 10 (CXCL10) levels in plasma samples was performed using LEGENDplex bead-based immunoassays (BioLegend) and FACSLyric flow cytometer (BD Biosciences). Data was analyzed using LEGENDplex analysis software v8.0.

**Statistics.** GraphPad Prism 5.0 (GraphPad Software Inc.) was used for statistical analyses. Normally distributed data were analyzed using the unpaired *t* test, whereas data that was not normally distributed was analyzed using the Mann-Whitney test, Spearman correlation and Wilcoxon matched-pairs signed rank test.

Accepted Manuscript

## RESULTS

**Patient characteristics.** We included 77 PCR confirmed COVID-19 patients with ARDS admitted to the ICU of the Erasmus MC, on average 2.0 (SD: ± 1.8) days after ICU admission, 6.4 (±4.8) days after hospitalization and 13.1 (±7.2) days after onset of disease (Table 1 and Supplementary Table 1). Patients were between 25 and 77 years old (mean: 63 ± 11.7 years), predominantly male (78%) and mostly had above normal BMI values (43% overweight and 40% obese). Thirty percent of patients did not have any known comorbidities. On average patients had moderately severe comorbid disease (Charlson Comorbidity Index: 2.8 ± 1.7), with the most common comorbidities being hypertension (32%), diabetes (28%), lung disease (22%) and cardiac disease (18%). At baseline (time of study inclusion), patients presented with critical COVID-19, indicated by the average Sequential Organ Failure Assessment (SOFA) score of 6.8 ± 2.9, and developed mild ARDS (10%), moderate ARDS (64%) or severe ARDS (24%) within the first 3 days of ICU admission, based on $PaO_2$:$FiO_2$ ratios (documented for 71 of 77 patients) and Berlin ARDS criteria [18]. During the course of infection 57% of patients developed thrombotic complications. At the end of the 30-day follow-up 54 (70%) patients were alive (released from the hospital: n = 29; clinical revalidation: n = 6; general ward: n = 7; ICU: n = 12) and 23 (30%) patients had died.

**Plasma NET levels correlate with viral load in sputum and neutrophil-recruiting chemokines in blood.** We determined the presence of NETs in plasma from 75 critically ill COVID-19 patients obtained at baseline (Supplementary Table 1), and 7 healthy control subjects. Plasma from COVID-19 patients contained significantly

Accepted Manuscript

elevated levels of histone-DNA (his-DNA) complexes ($p$=0.02), a commonly used surrogate marker for NETs [13, 19], and NET-specific MPO-DNA complexes ($p$<0.001) compared to healthy control subjects (Figure 1A). MPO-DNA levels correlated significantly with his-DNA abundance in plasma (Figure 1B) and with SARS-CoV-2 RNA load in paired sputum samples of COVID-19 patients (Figure 1C). Additionally, MPO-DNA levels correlated weakly with quantities of neutrophil-recruiting chemokines IL-8 and CXCL10 in plasma (Figure 1D). Thus, SARS-CoV-2-induced ARDS is associated with the presence of NETs in blood.

**Plasma NET levels peak early after ICU admission and correlate with inflammatory markers in critically ill COVID-19 patients.** To investigate the kinetics of plasma NET levels in relation to disease severity, we analyzed longitudinal plasma samples obtained from 29 COVID-19 patients requiring short ICU admission (<14 days; n=9), prolonged ICU admission ( ≥21 days; n=8) or with fatal disease (n=12). Plasma NET levels peaked early after ICU admission in the majority of patients (Figure 2A), irrespective of disease severity and/or outcome, and decreased over time gradually prior to release from ICU or death (Figure 2B). Furthermore, baseline NET abundance negatively correlated with the number of days after hospital admission (Figure 2C), indicating that NETs accumulate in plasma early after deterioration of disease and subsequent ICU admission.

Increased levels of inflammatory markers, including C-reactive protein (CRP), and pro-inflammatory cytokines such as IL-6 are present in blood of COVID-19 patients and are associated with disease severity [3, 4, 6]. We observed that plasma NET levels correlated with CRP and IL-6 levels in patients requiring prolonged ICU admission (Figure 2D), but not those released <14 days of ICU admission or with

Accepted Manuscript

fatal disease (Supplementary Figures 1A and 2A). Moreover, longitudinal changes of NET and CRP or IL-6 levels were similar in most COVID-19 patients requiring prolonged ICU admission (Figures 2D, Supplementary Figures 1 and 2), suggesting that inflammation and NET production are co-regulated.

**Baseline plasma NET levels correlate with disease severity, but not with development of thromboembolisms in critical COVID-19 patients.** Next, we investigated whether plasma NET abundance at baseline was associated with disease severity or development of thrombotic events in critically ill COVID-19 patients. Compared to surviving patients plasma NET levels correlated with overall disease severity (SOFA score) and severity of lung disease ($PaO_2/FiO_2$ ratio) in patients with fatal disease (Figure 3A). Forty-four (57%) patients developed thrombosis, including 41 patients with pulmonary embolism. Baseline plasma fibrinogen and D-dimer levels, but not platelet counts, were significantly higher in patients developing thrombosis (Supplementary Figure 3A). However, plasma NET levels at baseline and in longitudinal samples were not associated with development of thrombotic complications (Figure 3B and Supplementary Figure 3B). Moreover, plasma NET levels were not associated with fibrinogen nor platelet levels, and negatively correlated with D-dimer abundance (Figure 3C). Baseline NET levels were higher in samples obtained at longer interval from the thrombotic event (Supplementary Figure 3C), indicating that plasma NET abundance peaks early after hospitalization, whereas development of thrombotic complications generally occurs at later stages following ICU admission (median, range: 8, 1 – 22 days after ICU admission).

Accepted Manuscript

**NETs are produced and persist at high levels in lower respiratory tract samples of critically ill COVID-19 patients.** To investigate the presence of NETs in the lower respiratory tract (LRT) we analyzed surplus BL and BAL samples available from 21 critically ill COVID-19 patients (Supplementary Table 1), obtained on average 11.9 (± 7.1) days after study inclusion. Both his-DNA and MPO-DNA levels were significantly higher in LRT samples compared to blood samples from COVID-19 patients (Figure 4A). His-DNA and MPO-DNA levels in LRT samples correlated significantly (Spearman $r$ = 0.46, $p$ = 0.02). NET levels were similar between paired BAL samples obtained from bilateral BAL samples obtained at autopsy (Figure 4B), indicating that NETs are widely distributed in lungs of severe COVID-19 patients.

Paired LRT and blood samples were available for 19 patients. Notably, NET levels in paired blood and LTR samples did not correlate (Figure 4C). In contrast to plasma (Figure 2A), NET levels in longitudinal LRT samples (available for n = 8 patients) remained high and even increased over time in majority patients, especially in those who died from the disease (Figure 4D). To investigate the relationship between virus replication and presence of NETs in lungs of COVID-19 patients, SARS-CoV-2 specific RT-qPCR was performed on BAL and BL samples from 16 patients. SARS-CoV-2 RNA was detected in samples obtained early (mean ± SD: 9.5 ± 3.5 days), but not at later times after ICU admission (mean ± SD: 20.4 ± 5.4 days), with a median viral load of $2.0x10^6$ viral RNA copies/ml (range: $3.0x10^4$ – $1.4 x10^7$). Collectively, the data indicate that NETs are abundantly produced and persist in lungs of critically ill COVID-19 patients, even after virus replication has ceased.

Accepted Manuscript

**Neutrophils infiltrate and undergo NETosis in the lung of deceased COVID-19 patients with ARDS.** To substantiate our NET analyses on LRT samples, we analyzed lung tissue from 6 deceased COVID-19 patient with ARDS (Supplementary Table 1) for the presence of NETs. Consistent with our detection of SARS-CoV-2 RNA at early, but not at later times after ICU admission, *in situ* staining showed expression of SARS-CoV-2 nucleocapsid protein in 1  6 donors (Supplementary Figure 4). Citrullination of histone H3 (H3Cit) is an early step in NETosis, which ultimately leads to release of NETs characterized by aggregates of DNA, MPO and H3Cit in tissue sections [13]. Consistent with our detection of high NET levels in BL and BAL samples, abundant $MPO^{+}H3Cit^{+}$ neutrophils were observed in affected post-mortem lung tissue of all deceased COVID-19 patients examined (Figure 5A). Whereas $MPO^{+}H3Cit^{+}$ neutrophils were found in pulmonary vasculature, bronchi and alveoli, filamentous NETs were mainly observed in alveolar spaces (Figure 5B). We observed highly variable numbers of $CD61^{+}$ platelets, with occasional colocalization of $H3Cit^{+}$ neutrophils and $CD61^{+}$ platelets (Figure 6A). However, the majority of $MPO^{+}H3Cit^{+}$ neutrophils and NETs colocalized with fibrinogen depositions in bronchi and alveoli (Figure 6B). Thus, neutrophils infiltrate and undergo NETosis in lung during SARS-CoV-2 induced ARDS.

**DISCUSSION**

In this prospective cohort study we measured the levels of NETs in the lower respiratory tract and blood of critically ill COVID-19 patients admitted to the ICU, and compared NET abundance to virological, immunological and clinical parameters. Three main findings are reported. First, we showed that NET levels in blood are increased in critical COVID-19 patients, especially early after ICU admission, and correlate with the viral RNA load in sputum and blood levels of neutrophil-recruiting

Accepted Manuscript

chemokines and inflammatory markers. Second, NET levels were more abundant in lower respiratory tract samples compared to plasma samples of COVID-19 patients and, importantly, were found to persist during ICU admission. Third, we observed that filamentous NETs were mainly present in the alveoli and bronchi, which often contained fibrinogen networks enclosing abundant neutrophils undergoing NETosis.

Presence of high quantities of NETs in the lungs contributes to viral and non-viral ARDS [10, 20]. NET components, including extracellular histones and granular proteins like neutrophil elastase and myeloperoxidase, impair the pulmonary epithelial-endothelial barrier by dysregulating epithelial and endothelial cell junctions or inducing cell death, resulting in the accumulation of proteinaceous oedema and inflammatory cells in alveoli [21-23]. Additionally, NETs induce macrophages to secrete proinflammatory cytokines and stimulate plasmacytoid dendritic cells (pDCs) to release type I IFN [24, 25], thereby exacerbating the alveolar inflammatory response. Conversely, degradation of NETs, using DNase treatment or pharmacological inhibition of NETosis, prevents damage to the alveolar epithelial-endothelial barrier, reduces pulmonary inflammation and improves survival in experimental animal models of bacterial and viral lung disease [10, 26]. Moreover, in murine models of influenza virus-induced ARDS, DNase treatment was shown to improve survival, whereas excessive NET formation was shown to induce ARDS [21, 27]. Our detection of high NET levels in the lower respiratory tract of critically ill COVID-19 patients, combined with the generic mechanisms by which NETs contribute to ARDS, suggest that NETs are likely a pathogenic feature of COVID-19 ARDS.

NETs have been implicated in pulmonary disease caused by a broad diversity of human viruses, including RNA viruses such as influenza A virus, respiratory

Accepted Manuscript

syncytial virus and more recently also SARS-CoV-2, as well as DNA viruses like varicella-zoster virus [12, 15, 20, 28-30]. Consistent with a role of NETs in exacerbating pulmonary pathology, high quantities of NETs are present in respiratory tract samples from severe COVID-19, influenza pneumonia and varicella pneumonia patients [12, 31]. Interestingly, NET abundance generally correlates poorly between paired plasma and LRT samples of these patients (Figure 4C) [12, 31], possibly related to our observation that most NETs were formed and retained in alveoli and bronchi of COVID-19 patients. Consequently, plasma NET abundance appears to be a better predictor for disease severity in influenza A virus and SARS-CoV-2 infections compared to LRT samples [14, 15, 30, 31].

Coagulopathy is a prominent feature of severe COVID-19 and associated with poor prognosis [5]. NETosis and coagulation are intimately related, with each process capable of promoting the other [23, 32]. Detection of platelet-neutrophil aggregates in blood and microthrombi in affected lung tissue of COVID-19 patients suggest that neutrophils and/or NETs may contribute to SARS-CoV-2 induced coagulopathy [14]. This may involve NET components like extracellular histones, which have been described to cause platelet aggregation [33, 34]. We report that the longitudinal changes of plasma NET levels are not associated with thrombotic events, nor with soluble markers of thrombosis (i.e. fibrinogen, D-dimer and platelet counts); the latter was also observed by *Middleton et al.* [14]. Nevertheless, pulmonary microthrombi are already present in early stages of some COVID-19 [35], and may capture and activate primed neutrophils to release NETs [14]. Similar to a recent report [28] we observed that NETs were predominantly located in bronchioles and alveoli. By contrast, the pulmonary vasculature contained many $H3Cit^{+}$ neutrophils [14, 28], but not NETs, suggesting that neutrophils may be primed by

Accepted Manuscript

pulmonary microthrombi and only undergo complete NETosis upon release into the fibrinogen-rich alveolar space [36].

Regulated NETosis may contribute to the host immune defence against SARS-CoV-2 infection in asymptomatic or mild cases, e.g. by physically entrapping viral particles and reducing virus replication [20, 37]. Factors contributing to severe COVID-19, including SARS-CoV-2 load in the respiratory tract and levels of proinflammatory cytokines in blood [6, 38], may concurrently stimulate excessive NET production [11, 13]. Consistent with SARS-CoV-2 induced NETosis, we found that plasma NET levels positively correlated with viral RNA load in sputum samples. Additionally, we observed that NET levels positively correlated with inflammatory markers in blood of critically ill COVID-19 patients, suggesting that circulating cytokines may trigger NETosis. Indeed, serum of COVID-19 patients – containing high quantities of cytokines [4, 6] – was previously shown to induces NETosis in neutrophils of healthy subjects [15].

A limitation of this study, and previous studies [14, 15], is that only hospitalized patients were analyzed, whereas the majority of SARS-CoV-2 infected individuals develop mild disease [39, 40]. Additionally, the BL and BAL samples analyzed were all obtained from critically ill COVID-19 patients, for diagnostic purposes, at the time of severe lung disease, but not were not available at the convalescent phase of the disease. It will be important to compare plasma NET abundance in non-hospitalized and hospitalized COVID-19 patients of variable disease severity to dissect the beneficial versus pathogenic roles of NETs in SARS-CoV-2 infected individuals.

Accepted Manuscript

Collectively, the data demonstrate that NETs are present in blood and, especially the lower respiratory tract of critically ill COVID-19 patients. The persisting high levels of NETs in the lower respiratory tract of severe COVID-19 patients and the well-established role of aberrant NET formation in ARDS support the current clinical trials (NCT04359654; NCT04409925) that currently investigate the therapeutic value of targeting NETs to improve outcome of disease in COVID-19 patients.

Accepted Manuscript

## FUNDING

The department of Viroscience received support from the EU Horizon 2020 dedicated call for COVID-19 research, grant number 101003589 (RECOVER). The department of Pathology received support from ZonMw grant number 10430 01 201 0016.

## ACKNOWLEDGMENTS

We thank Katharina S. Schmitz, David A.M.C. van de Vijver, Mart Lamers, Debby Schipper, Ditty van Duijn, Patricia Ormskerk and Melanie Glasbergen – van Beijeren for their contributions to this study.

## CONFLICTS OF INTERESTS

The authors have no conflicts of interest to declare.

Accepted Manuscript

## REFERENCES


1. Zhou P, Yang XL, Wang XG, et al. A pneumonia outbreak associated with a new coronavirus of probable bat origin. Nature **2020**; 579:270-3.

2. Dong E, Du H, Gardner L. An interactive web-based dashboard to track COVID-19 in real time. Lancet Infect Dis **2020**; 20:533-4.

3. Guan WJ, Ni ZY, Hu Y, et al. Clinical Characteristics of Coronavirus Disease 2019 in China. N Engl J Med **2020**; 382:1708-20.

4. Huang C, Wang Y, Li X, et al. Clinical features of patients infected with 2019 novel coronavirus in Wuhan, China. Lancet **2020**; 395:497-506.

5. Klok FA, Kruip M, van der Meer NJM, et al. Incidence of thrombotic complications in critically ill ICU patients with COVID-19. Thromb Res **2020**; 191:145-7.

6. Mehta P, McAuley DF, Brown M, et al. COVID-19: consider cytokine storm syndromes and immunosuppression. Lancet **2020**; 395:1033-4.

7. Barnes BJ, Adrover JM, Baxter-Stoltzfus A, et al. Targeting potential drivers of COVID-19: Neutrophil extracellular traps. J Exp Med **2020**; 217.

8. Matthay MA, Zemans RL, Zimmerman GA, et al. Acute respiratory distress syndrome. Nat Rev Dis Primers **2019**; 5:18.

9. Brinkmann V, Reichard U, Goosmann C, et al. Neutrophil extracellular traps kill bacteria. Science **2004**; 303:1532-5.

10. Lefrancais E, Mallavia B, Zhuo H, Calfee CS, Looney MR. Maladaptive role of neutrophil extracellular traps in pathogen-induced lung injury. JCI Insight **2018**; 3.

11. Schonrich G, Raftery MJ. Neutrophil Extracellular Traps Go Viral. Front Immunol **2016**; 7:366.

12. Ouwendijk WJ, van den Ham HJ, Delany MW, et al. Alveolar barrier disruption in varicella pneumonia is associated with neutrophil extracellular trap formation. JCI Insight **2020**.


Accepted Manuscript

13. Jorch SK, Kubes P. An emerging role for neutrophil extracellular traps in noninfectious disease. Nat Med **2017**; 23:279-87.

14. Middleton EA, He XY, Denorme F, et al. Neutrophil Extracellular Traps (NETs) Contribute to Immunothrombosis in COVID-19 Acute Respiratory Distress Syndrome. Blood **2020**.

15. Zuo Y, Yalavarthi S, Shi H, et al. Neutrophil extracellular traps in COVID-19. JCI Insight **2020**; 5.

16. Jeroen J.A. van Kampen DAMCvdV, Pieter L.A. Fraaij, Bart L. Haagmans, Mart M. Lamers, Nisreen Okba, Johannes P.C. van den Akker, Henrik Endeman, Diederik A.M.P.J. Gommers, Jan J. Cornelissen, Rogier A.S. Hoek, Menno M. van der Eerden, Dennis A. Hesselink, Herold J. Metselaar, Annelies Verbon, Jurriaan E.M. de Steenwinkel, Georgina I. Aron, Eric C.M. van Gorp, Sander van Boheemen, Jolanda C. Voermans, Charles A.B. Boucher, Richard Molenkamp, Marion P.G. Koopmans, Corine Geurtsvankessel, Annemiek A. van der Eijk. Shedding of infectious virus in hospitalized patients with coronavirus disease-2019 (COVID-19): duration and key determinants. medRxiv **2020**.

17. Kessenbrock K, Krumbholz M, Schonermarck U, et al. Netting neutrophils in autoimmune small-vessel vasculitis. Nat Med **2009**; 15:623-5.

18. Force ADT, Ranieri VM, Rubenfeld GD, et al. Acute respiratory distress syndrome: the Berlin Definition. JAMA **2012**; 307:2526-33.

19. Ebrahimi F, Giaglis S, Hahn S, et al. Markers of neutrophil extracellular traps predict adverse outcome in community-acquired pneumonia: secondary analysis of a randomised controlled trial. Eur Respir J **2018**; 51.

20. Cortjens B, de Boer OJ, de Jong R, et al. Neutrophil extracellular traps cause airway obstruction during respiratory syncytial virus disease. J Pathol **2016**; 238:401-11.

21. Narasaraju T, Yang E, Samy RP, et al. Excessive neutrophils and neutrophil extracellular traps contribute to acute lung injury of influenza pneumonitis. Am J Pathol **2011**; 179:199-210.

Accepted Manuscript

22. Saffarzadeh M, Juenemann C, Queisser MA, et al. Neutrophil extracellular traps directly induce epithelial and endothelial cell death: a predominant role of histones. PLoS One **2012**; 7:e32366.

23. Caudrillier A, Kessenbrock K, Gilliss BM, et al. Platelets induce neutrophil extracellular traps in transfusion-related acute lung injury. J Clin Invest **2012**; 122:2661-71.

24. Warnatsch A, Ioannou M, Wang Q, Papayannopoulos V. Inflammation. Neutrophil extracellular traps license macrophages for cytokine production in atherosclerosis. Science **2015**; 349:316-20.

25. Papayannopoulos V. Neutrophil extracellular traps in immunity and disease. Nat Rev Immunol **2018**; 18:134-47.

26. Toussaint M, Jackson DJ, Swieboda D, et al. Host DNA released by NETosis promotes rhinovirus-induced type-2 allergic asthma exacerbation. Nat Med **2017**; 23:681-91.

27. Pillai PS, Molony RD, Martinod K, et al. Mx1 reveals innate pathways to antiviral resistance and lethal influenza disease. Science **2016**; 352:463-6.

28. Radermecker C, Detrembleur N, Guiot J, et al. Neutrophil extracellular traps infiltrate the lung airway, interstitial, and vascular compartments in severe COVID-19. J Exp Med **2020**; 217.

29. Zhang JJY, Lee KS, Ang LW, Leo YS, Young BE. Risk Factors of Severe Disease and Efficacy of Treatment in Patients Infected with COVID-19: A Systematic Review, Meta-Analysis and Meta-Regression Analysis. Clin Infect Dis **2020**.

30. Zhu L, Liu L, Zhang Y, et al. High Level of Neutrophil Extracellular Traps Correlates With Poor Prognosis of Severe Influenza A Infection. J Infect Dis **2018**; 217:428-37.

31. Zhang N, Zhu L, Zhang Y, et al. Circulating Rather Than Alveolar Extracellular Deoxyribonucleic Acid Levels Predict Outcomes in Influenza. J Infect Dis **2020**; 222:1145-54.

32. Fuchs TA, Brill A, Duerschmied D, et al. Extracellular DNA traps promote thrombosis. Proc Natl Acad Sci U S A **2010**; 107:15880-5.

Accepted Manuscript

33. Ashar HK, Mueller NC, Rudd JM, et al. The Role of Extracellular Histones in Influenza Virus Pathogenesis. Am J Pathol **2018**; 188:135-48.

34. Fuchs TA, Bhandari AA, Wagner DD. Histones induce rapid and profound thrombocytopenia in mice. Blood **2011**; 118:3708-14.

35. Polak SB, Van Gool IC, Cohen D, von der Thusen JH, van Paassen J. A systematic review of pathological findings in COVID-19: a pathophysiological timeline and possible mechanisms of disease progression. Mod Pathol **2020**.

36. Oehmcke S, Morgelin M, Herwald H. Activation of the human contact system on neutrophil extracellular traps. J Innate Immun **2009**; 1:225-30.

37. Saitoh T, Komano J, Saitoh Y, et al. Neutrophil extracellular traps mediate a host defense response to human immunodeficiency virus-1. Cell Host Microbe **2012**; 12:109-16.

38. Zheng S, Fan J, Yu F, et al. Viral load dynamics and disease severity in patients infected with SARS-CoV-2 in Zhejiang province, China, January-March 2020: retrospective cohort study. BMJ **2020**; 369:m1443.

39. Kluytmans-van den Bergh MFQ, Buiting AGM, Pas SD, et al. Prevalence and Clinical Presentation of Health Care Workers With Symptoms of Coronavirus Disease 2019 in 2 Dutch Hospitals During an Early Phase of the Pandemic. JAMA Netw Open **2020**; 3:e209673.

40. Pollan M, Perez-Gomez B, Pastor-Barriuso R, et al. Prevalence of SARS-CoV-2 in Spain (ENE-COVID): a nationwide, population-based seroepidemiological study. Lancet **2020**.

Accepted Manuscript

## FIGURE LEGENDS

**Figure 1.** Plasma NET levels correlate with viral load in sputum and neutrophil-recruiting chemokines in blood. (A) Absorbance values (450 nm – 620 nm) of his-DNA and MPO-DNA ELISAs performed on plasma samples from 7 healthy controls (HC) and 75 critically ill COVID-19 patients. Horizontal line indicates median. (B) Correlation between his-DNA and MPO-DNA abundance (absorbance units; AU) in plasma samples of 75 COVID-19 patients. (C) Correlation between SARS-CoV-2 RNA load in sputum and the MPO-DNA abundance in paired plasma samples. (D) Correlation between MPO-DNA abundance and IL-8 or CXCL10 quantity in plasma samples, as determined by ELISA and LEGENDplex assay. (B – D) Spearman r and *p*-values are indicated.

**Figure 2.** Plasma NET levels peak early after ICU admission and correlate with inflammation markers in plasma of critically ill COVID-19 patients. (A) MPO-DNA abundance (absorbance units; AU) was determined by ELISA on serial plasma samples of COVID-19 patients requiring short ICU admission (<14 days; n = 9), long ICU admission (≥ 21 days; n = 8) or patients with fatal disease (n = 12). Red symbol: peak MPO-DNA abundance for each patient. (B) Comparison between peak MPO-DNA abundance and MPO-DNA levels on the last sample taken prior to release from the ICU or death. Wilcoxon matched-pairs signed rank test *p*-values are indicated. (C) Correlation between MPO-DNA level and time after hospitalization. (D) Correlation between MPO-DNA and CRP or IL-6 abundance. Graphs of two representative (out of eight) severe COVID-19 patients are included (CRP: CIUM-166; IL-6: CIUM-139), showing CRP and IL-6 levels (left *Y*-axis; blue) and MPO-DNA

Accepted Manuscript

abundance (right *Y*-axis; pink) in sequential plasma samples. Spearman r and *p*-value are indicated.

**Figure 3.** Baseline plasma NET levels correlate with disease severity, but not development of thromboembolisms in critically ill COVID-19 patients. (A) Correlation between MPO-DNA abundance (absorbance units; AU) in plasma of COVID-19 patients requiring short ICU admission (<14 days; n = 15), long ICU admission (≥ 21 days; n = 28) or patients with fatal disease (n = 21) and the SOFA score or $PaO_2/FiO_2$ ratio. (B) Comparison of MPO-DNA abundance in plasma at baseline between patients that developed thrombotic complications (n=44) or did not develop thrombosis (n=33). Horizontal line indicates median. (C) Correlation between MPO-DNA abundance (AU) and fibrinogen and D-dimer levels, and platelet count in plasma of COVID-19 patients that developed thromboembolisms (fibrinogen/D-dimer: n = 37; platelets: n = 33) or did not develop thrombosis (fibrinogen/D-dimer: n = 21; platelets: n = 32). Spearman r and *p*-value are indicated.

**Figure 4.** NETs are produced and persist at high levels in lower respiratory tract samples of critically ill COVID-19 patients. His-DNA and MPO-DNA abundance (absorbance units; AU) was determined by ELISA. (A) His-DNA and MPO-DNA levels in blood samples from healthy controls (HC; n = 7) and COVID-19 patients (29 samples from 19 patients), and lower respiratory tract (LRT: BAL or BL) samples from severe COVID-19 patients (37 samples from 21 patients). Patients with ARDS caused by influenza A virus (IVA; n = 2) and lung transplant patients (LTx; n = 2) were included as positive and negative controls, respectively. Horizontal line indicates median. (B) MPO-DNA levels in paired BAL samples obtained at autopsy

Accepted Manuscript

from left and right lung lobes. (C) No correlation between MPO-DNA levels in paired LRT and blood samples (n = 19 patients). Spearman r and *p*-value are indicated. (D) Analysis of sequential LRT samples available for 8 patients (left panel), 5 of which did not survive the disease (right panel).

**Figure 5.** Neutrophils infiltrate and undergo NETosis in the lung of deceased COVID-19 patient with ARDS. Lung tissue from 6 COVID-19 patients was stained with hematoxylin and eosin or double immunohistochemically stained for MPO (red) and citrullinated histone H3 (H3Cit; blue). (A) Representative images of MPO-H3Cit staining in the pulmonary vasculature (CIUM-173), bronchioles (CIUM-162) and alveoli (CIUM-146). Scale bars indicate 100 µm (vasculature and bronchi: top and middle row, respectively) and 50 µm (vasculature and bronchi: bottom row; alveoli: all panels). (B) Representative images of filamentous NETs in alveoli of deceased COVID-19 patients with ARDS (from top to bottom: CIUM-122, CIUM-160 and CIUM-146). Scale bars indicate 50 µm. (A and B) Enlargements of areas indicated by black boxes are shown.

**Figure 6.** Neutrophils undergoing NETosis co-localize with fibrinogen in the bronchi and alveoli of deceased COVID-19 patient with ARDS. Lung tissue from 6 COVID-19 patients was stained with hematoxylin and eosin or double immunohistochemically stained for (A) H3Cit (red) and CD61 (blue) or (B) H3Cit (red) and fibrinogen (blue). Representative images are shown for H3Cit-CD61 staining (CIUM-160) and H3Cit-fibrinogen staining (alveoli: CIUM-122; bronchi: CIUM-162). (A) Scale bars indicate 50 µm and 100 µm (enlargement). (B) Scale bars indicate 100 µm and 50 µm (enlargements). (A and B) Enlargement of areas indicated by black boxes is shown.

Accepted Manuscript

## TABLE

### Table 1. COVID-19 patient characteristics

| | |
|---|---|
| **General** | |
| Number | 77 |
| Age (mean ± SD) | 63·0 ± 11·7 |
| Sex | |
| Male | 78% |
| Female | 22% |
| Time after hospitalization (days; mean ± SD)[a] | 6·4 ± 4·8 |
| Time after ICU admission (days; mean ± SD)[a] | 2·0 ± 1·8 |
| Time after onset of disease (days; mean ± SD)[a] | 13·1 ± 7·2 |
| BMI | |
| ≤18.5 (underweight) | 1% |
| 18.5 – 24.9 (normal) | 16% |
| 25.0 – 29.9 (overweight) | 43% |
| ≥30 (obese) | 40% |
| SOFA score (mean ± SD) [a] | 6·8 ± 2·9 |
| $PaO_2$:$FiO_2$ ratio[b] | |
| ≤100 | 10% |
| 101 – 200 | 64% |
| 201 – 300 | 24% |
| >300 | 3% |
| **Comorbidities** | |
| CMI (mean ± SD) | 2·8 ± 1·7 |
| Cancer | 10% |
| Cardiac disease | 18% |
| Diabetes | 27% |
| Hypertension | 31% |
| Lung disease | 22% |

Accepted Manuscript

| | |
|---|---|
| Neurological disease | 5% |
| Renal disease | 3% |
| Vascular disease | 5% |
| **Laboratory findings**[a] | |
| C-reactive protein (mg/L; mean ± SD) | 265 ± 143 |
| Lactate dehydrogenase (U/L; mean ± SD) | 360 ± 169 |
| Interleukin-6 (pg/mL; mean ± SD) | 328 ± 815 |
| Platelet count ($10^9$/L; mean ± SD) | 311 ± 129 |
| Leukocyte count ($10^9$/L; mean ± SD) | 9·6 ± 4·8 |
| Ferritin (µg/mL; mean ± SD) | 1998 ± 1421 |
| Fibrinogen (g/L; mean ± SD) | 7·2 ± 1·9 |
| D-dimer (mg/L; mean ± SD) | 5·8 ± 8·8 |
| **Outcome** | |
| Thrombo-embolism during ICU admission | 57% |
| 30-day survival | 73% |

[a]Baseline (time of study inclusion). [b]Minimum median $PaO_2$:$FiO_2$ ratio in first 3 days of study inclusion.

Accepted Manuscript

Figure 1

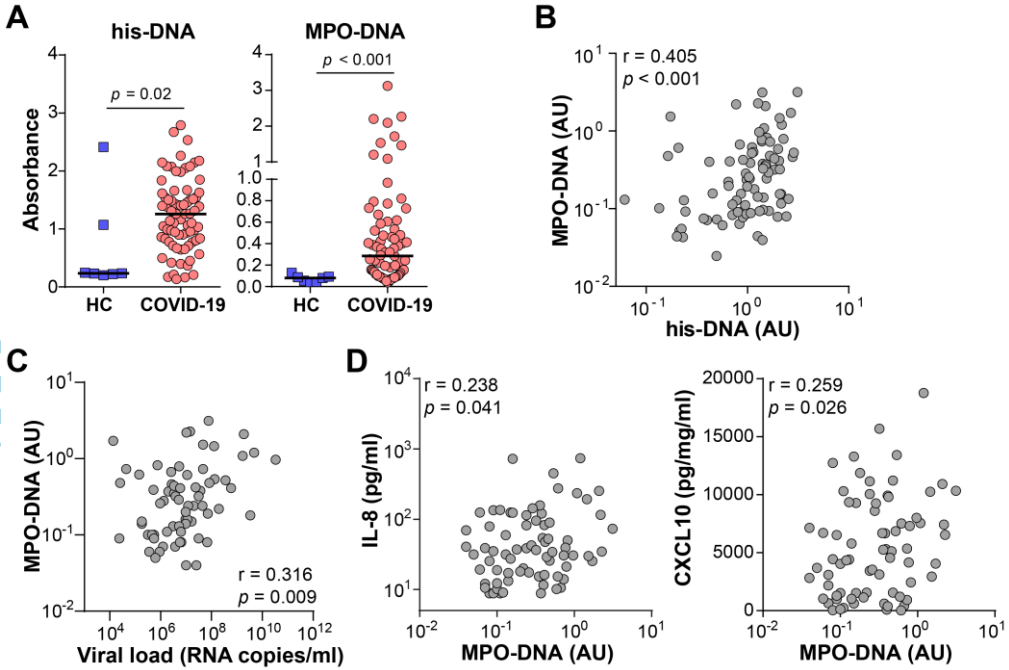


Accepted Manuscript

Figure 2

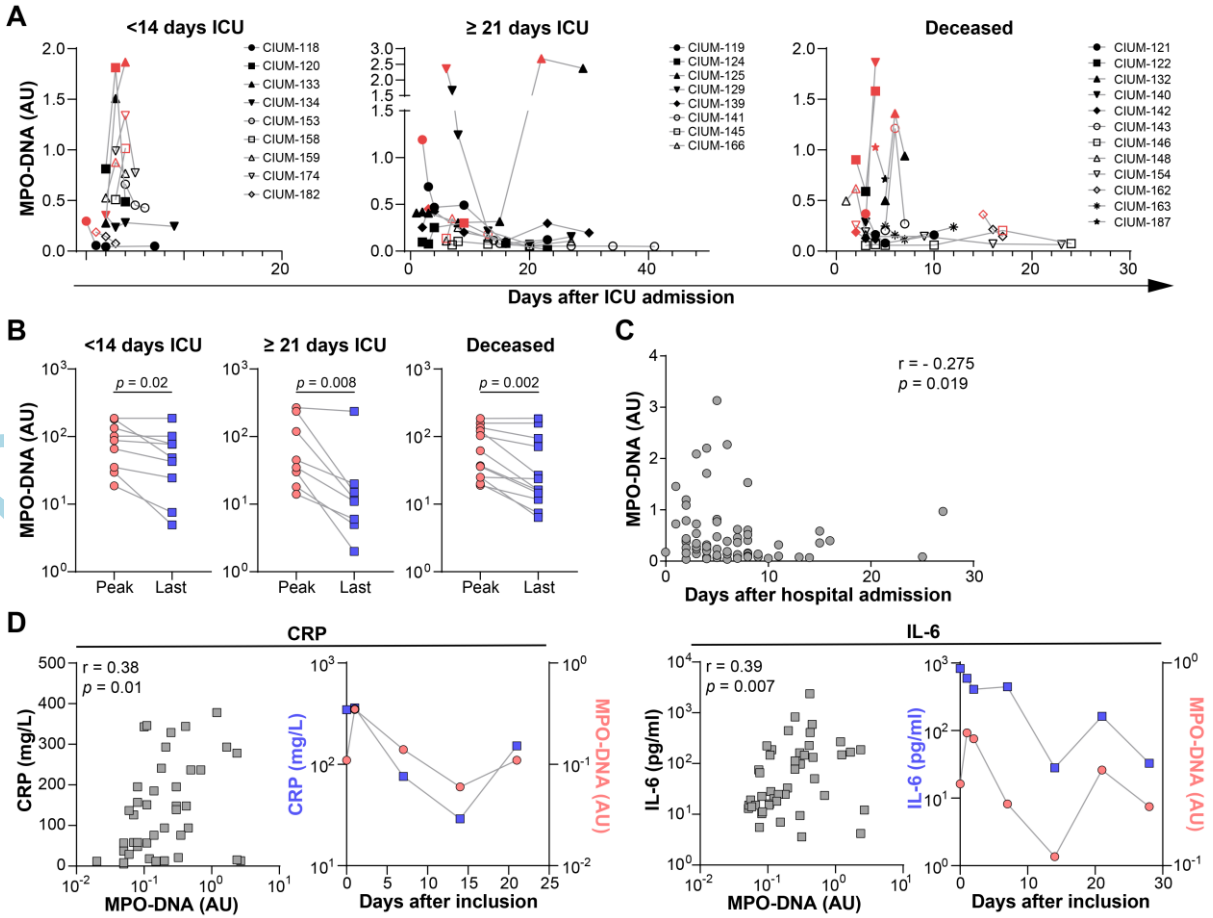
A
<14 days ICU
≥ 21 days ICU
Deceased
MPO-DNA (AU)
CIUM-118
CIUM-120
CIUM-133
CIUM-134
CIUM-153
CIUM-158
CIUM-159
CIUM-174
CIUM-182
CIUM-119
CIUM-124
CIUM-125
CIUM-129
CIUM-139
CIUM-141
CIUM-145
CIUM-166
CIUM-121
CIUM-122
CIUM-132
CIUM-140
CIUM-142
CIUM-143
CIUM-146
CIUM-148
CIUM-154
CIUM-162
CIUM-163
CIUM-187
Days after ICU admission
B
<14 days ICU
≥ 21 days ICU
Deceased
p = 0.02
p = 0.008
p = 0.002
MPO-DNA (AU)
Peak
Last
C
r = - 0.275
p = 0.019
MPO-DNA (AU)
Days after hospital admission
D
CRP
r = 0.38
p = 0.01
CRP (mg/L)
MPO-DNA (AU)
Days after inclusion
IL-6
r = 0.39
p = 0.007
IL-6 (pg/ml)
MPO-DNA (AU)
Days after inclusion

Figure 3

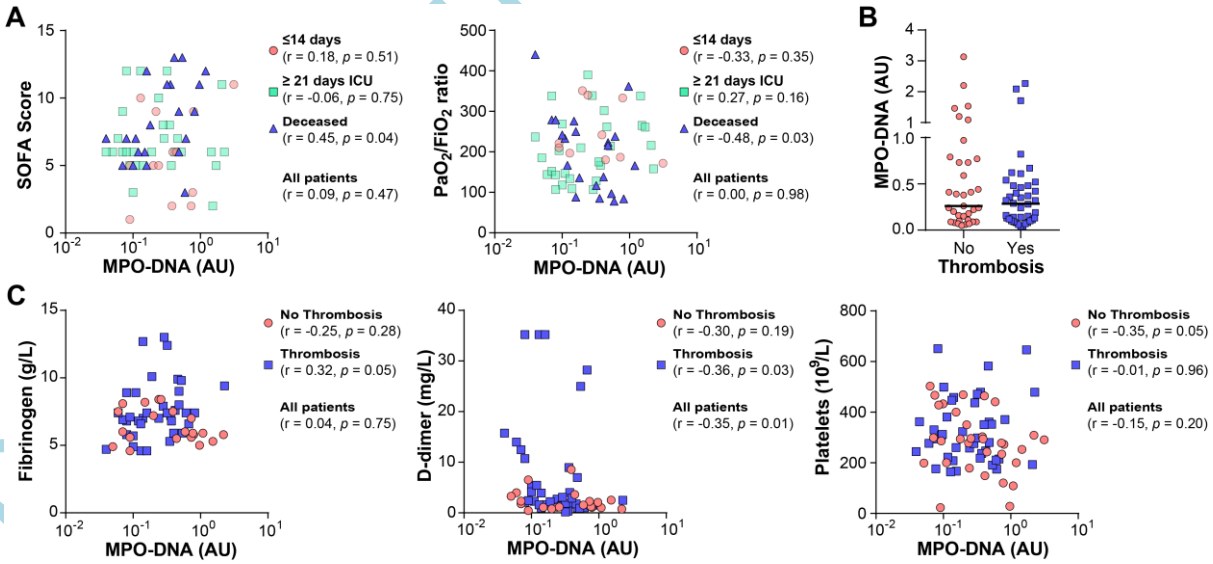
A
SOFA Score
MPO-DNA (AU)
≤14 days
(r = 0.18, p = 0.51)
≥ 21 days ICU
(r = -0.06, p = 0.75)
Deceased
(r = 0.45, p = 0.04)
All patients
(r = 0.09, p = 0.47)
PaO2/FiO2 ratio
MPO-DNA (AU)
≤14 days
(r = -0.33, p = 0.35)
≥ 21 days ICU
(r = 0.27, p = 0.16)
Deceased
(r = -0.48, p = 0.03)
All patients
(r = 0.00, p = 0.98)
B
MPO-DNA (AU)
No
Yes
Thrombosis
C
Fibrinogen (g/L)
MPO-DNA (AU)
No Thrombosis
(r = -0.25, p = 0.28)
Thrombosis
(r = 0.32, p = 0.05)
All patients
(r = 0.04, p = 0.75)
D-dimer (mg/L)
MPO-DNA (AU)
No Thrombosis
(r = -0.30, p = 0.19)
Thrombosis
(r = -0.36, p = 0.03)
All patients
(r = -0.35, p = 0.01)
Platelets (10^9/L)
MPO-DNA (AU)
No Thrombosis
(r = -0.35, p = 0.05)
Thrombosis
(r = -0.01, p = 0.96)
All patients
(r = -0.15, p = 0.20)

Figure 4

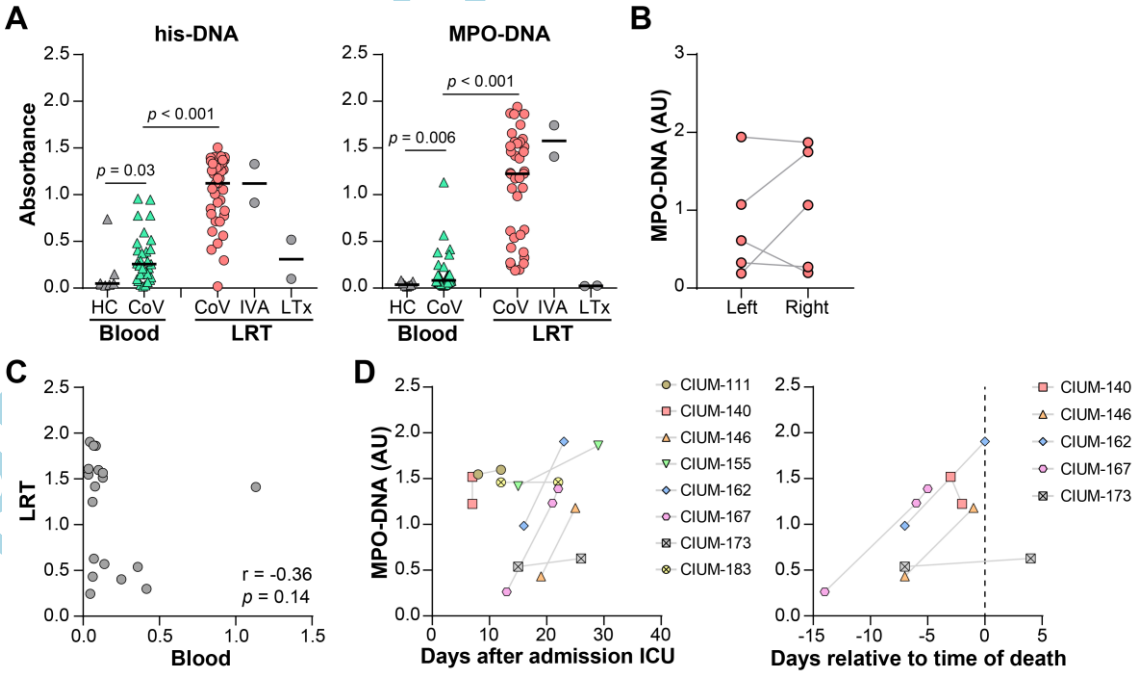


Accepted Manuscript

Figure 5

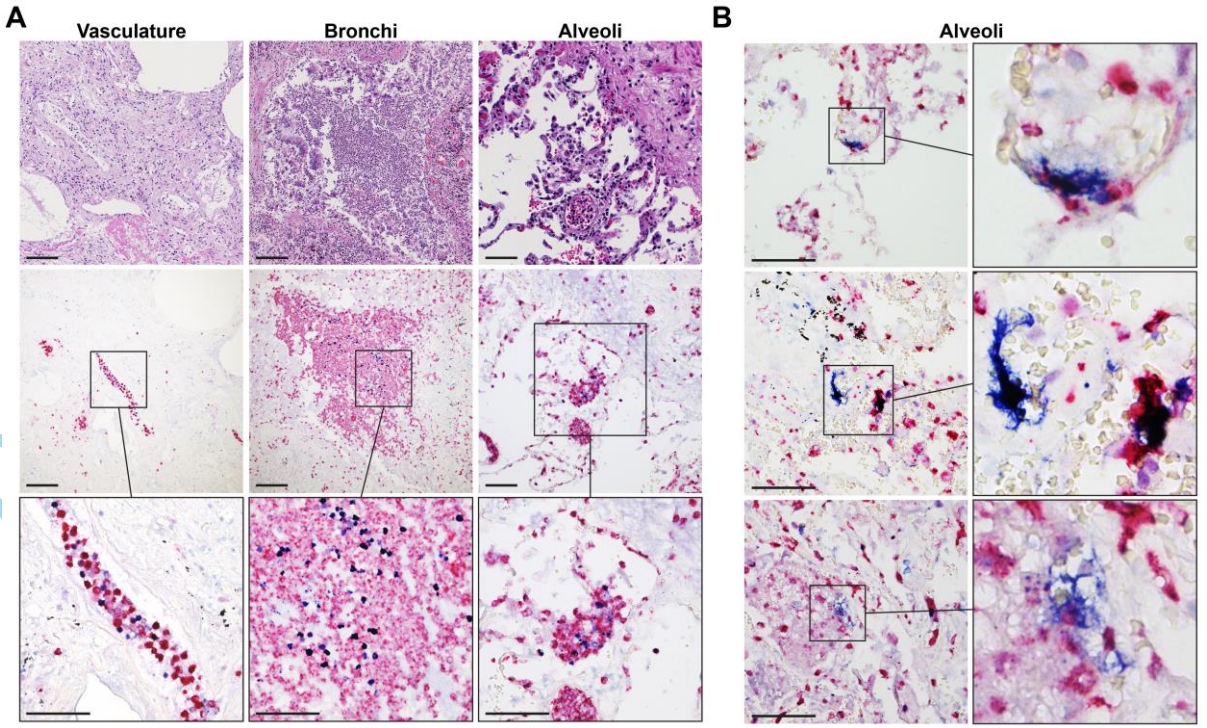


Accepted Manuscript

Figure 6

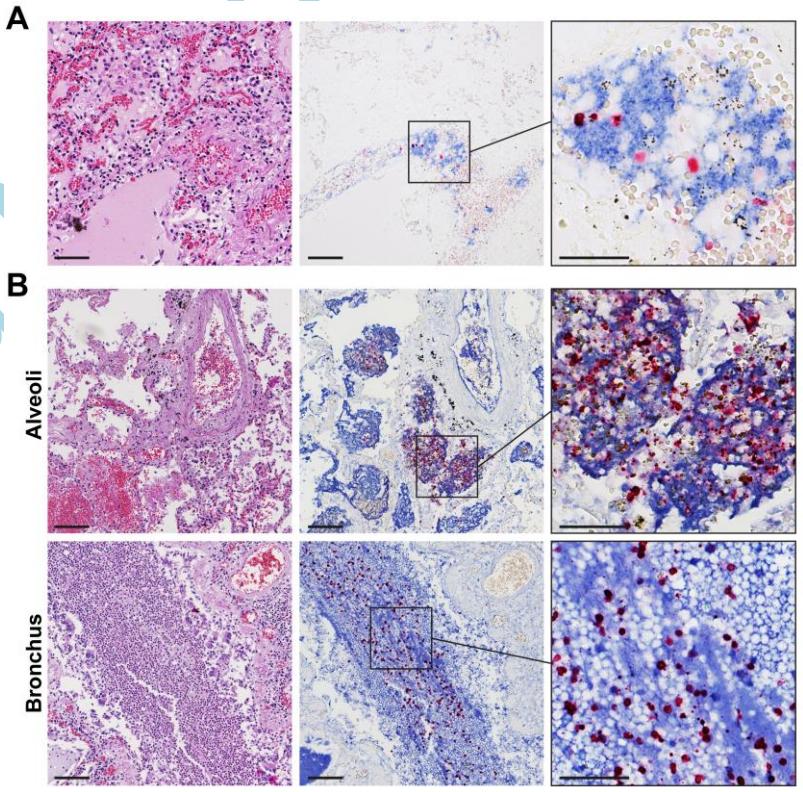


Accepted Manuscript